

# Spatiotemporal monitoring of natural objects in occluded scenes by means of a robotic multi-sensor system

*Dr.-Ing. Jens-André Paffenzahl<sup>1</sup>, M.Sc. Corinna Harmening<sup>2</sup>*

*<sup>1</sup>Geodetic Institute, Leibniz Universität Hannover*

*<sup>2</sup>Department of Geodesy and Geoinformation, Research Group Engineering Geodesy, Vienna University of Technology*

## Abstract

This contribution deals with the **spatiotemporal monitoring of natural objects**, like plants under canopy conditions. The superior goal is the characterization of the plant's behavior over time in terms of growths and short-term morphological adaptations. To reach this goal an **automated data acquisition** is required, which can be easily scaled in time. Therefore, a **robotic multi-sensor system** is designed to pave the way for a semi-automated data acquisition. The base of the multi-sensor system is a small-scale robot of type Volksbot RT6 by Fraunhofer IAIS. The main sensor for the 3-dimensional data acquisition is a laser scanner of type SICK LMS500. The multi-sensor system is enhanced with a second laser scanner, a digital camera and a low-cost GPS aided MEMS based IMU. This allows the acquisition of the entire plant by means of well-distributed survey positions. With this setup, experiments for a model plant, the cucumber, were carried out in a greenhouse facility. Results for **time series of 3D point clouds** of a cucumber plant will be presented.

Two main steps of the processing chain are discussed in detail. First, the **referencing** of the individual survey positions to provide a 3D point cloud in a common coordinate system for each epoch as well as to link the different epochs. Here, a priori information about the survey positions is considered. Afterwards, iterative matching algorithms are applied to stable areas of the point cloud over time to link different epochs. Second, the **3D point cloud segmentation** of the natural plant objects is treated. Besides occlusions, contacts of plant leaves are the most challenging tasks to solve. An efficient **graph-based segmentation algorithm** is refined to obtain an initial segmentation of each epoch. Subsequently, a **shape matching** is used to improve the result as well as to track the regions over time. Finally, segmented leaves of subsequent epochs with links between each other are available as result of the spatiotemporal segmentation.

## Keywords

laser scanner, data fusion, referencing, 3d point cloud, segmentation, shape matching

## 1 MOTIVATION

The challenge of spatiotemporal monitoring of natural objects, in particular of plants under canopy conditions, is twofold: On the one hand, a proper 3D acquisition method is demanded which can be applied in narrow and cluttered greenhouse environments with a certain degree of automation and referencing capabilities. On the other hand, a sophisticated data analysis is required to handle occlusions and contacts of plant leaves in the 3D data and the subsequent analysis of geometrical plant traits. Also the analysis should account for time series of 3D data to pave the way for monitoring purposes.

*Why should the data acquisition be performed in narrow and cluttered greenhouse environments?*

The main reason is the difference of plants' morphological phenotypes between plants grown individually or under canopy conditions close to actual practise. The phenotypic plasticity of the plants affects the productivity due to short and long term adaptations of the plants' physiological functions. These interactions make structural plant analysis a key field of studies in plant science studies (FIORANI & SCHURR, 2013). The size, shape and orientation of the leaves are the key parameters for

above ground plant parts (KLOSE ET AL., 2009) as they are the major place of photosynthetic activity and therefore influence productivity strongly.

*What are the reasons for a spatiotemporal monitoring?*

In plant breeding phenotyping has gained increased importance as advances in genotyping and quantitative analysis of the plant traits allow to establish new and more efficient technologies for plant breeding (WHITE ET AL., 2012; FIORANI & SCHURR, 2013). Especially for the analysis of genotype, environment and the interaction of both high throughput phenotyping methods with a high degree of automatism are needed. A high temporal resolution is also needed when short-term tropism are under consideration. The short-term movements also interact with the long-term morphological adaptation to abiotic stresses induced by e. g. drought or salinity.

Aforementioned topics require alternative methods compared to the frequently used destructive measurements by means of area meters as well as the non-destructive manual digitization of characteristic points of the plant organs by means of electromagnetic digitizers (e. g. KAHLEN & STÜTZEL, 2007). Essentials for the alternative method are an automated contact-free data acquisition with an increased spatial and temporal resolution along with a sophisticated extraction and modeling of the individual plant organs out of 3D data.

## **2 RELATED WORK**

The contact-free and automated monitoring of plant populations by means of photogrammetric images and the laser scanning technique is investigated by various research groups with different objectives. BUSEMEYER ET AL. (2013) introduce a multi-sensor platform for non-destructive field-based phenotyping for small grain cereals. The sensor platform is equipped with various sensor types, like 3D time-of-flight cameras, digital cameras, laser distance sensors as well as hyperspectral and light curtain imaging. ROSELL ET AL. (2009) and SANZ-CORTIELLA ET AL. (2011) use 2D laser scanners installed on a tractor to determine geometric (e. g. height, volume) and structural (e. g. leaf area index (LAI)) parameters of plants in orchards. SELBECK ET AL. (2010) use a 2D automotive laser scanner mounted on a tractor to determine parameters of grain populations under field conditions. HOFFMEISTER ET AL. (2012) make use of a terrestrial laser scanner mounted on a tractor to determine the biomass and LAI of sugar beets. NORZAHARI ET AL (2011) introduce a mobile platform equipped with a 2D laser scanner for inventory purposes of a wine yard. Common for all aforementioned approaches is their automated laser-based data acquisition of plant populations in the open field. Typically, this results in a decreased resolution of the individual plants and thus a limitation to specific choice of plant parameters. HÖFLE (2013) proposes a novel workflow for an individual maize plant detection using terrestrial laser scanner point clouds. The author uses a static ground-based full-waveform laser scanner and in the analysis besides the geometric as well as the radiometric data is involved. A data-driven radiometric correction procedure of the 3D point cloud is proposed. Results and evaluation of the radiometric correction, the plant detection and analysis of the effect of the point density on the detection procedure are presented in detail.

Approaches on plant measurement include ALENYA ET AL. (2011), who present a proof-of-concept approach to robotized plant measuring. Plant leaves are modeled by fusing dense color and sparse depth data acquired by the Time-of-Flight cameras mounted on a mock-up measurement robot arm. Works on individual plants include GORTE & PFEIFER (2004), in which the laser points are rasterized in 3D voxel space and operations such as closing from mathematical morphology and thinning are used to obtain a connected 3D skeleton. GORTE & WINTERHALDER (2004) further segment the remaining voxels into different branches and finally, branch labels are assigned to the original laser points. The approach presented by SUN ET AL. (2011) focuses on the extraction of venation and contour of individual flatwise placed leaves from point cloud data. A contribution to the classification of plant organs by means of point clouds acquired with a precise close range laser scanner is given by PAULUS ET AL. (2013). The authors use a surface feature histogram based approach to classify grapevine stems and leaves as well as wheat ears from other plant organs.

UHRMANN ET AL. (2011) present a system design and data processing for the sheet-of-light measurement method for plant phenotyping. Sheet-of-light measurement works based on the triangulation principle with the diffuse reflection of the laser line captured by the camera and deliver height profile of the target object for automatic determination of the morphological plant features. The shadowing and occlusion, however, are main issues of this scheme. PAPROKI ET AL. (2012) present a mesh based analysis of vegetative growth. Plant meshes are previously reconstructed from multi-view images as the input data. Morphological mesh segmentation, phenotypic parameter estimation, and plant organs tracking over time are conducted on cotton plants over four time-points. SEATOVIC (2013) presents his work on methods for real-time plant detection. His aim is to provide a reliable plant detection system and algorithm based on leaf shapes. He proposes to use a sample database for the leaves which should be used in the detection algorithm. In his experimental acquisition system a laser triangulation sensor is used.

### 3 GENERATION OF THE TIME SERIES OF 3D POINT CLOUDS

This section introduces the robotic multi-sensor system, which is used for the data acquisition, and outlines the data pre-processing. Afterwards, the focus is on the required referencing task. A common coordinate system for the different survey positions within a single epoch is established within the spatial referencing (also called registration) step. This step can be separated into a coarse registration and a fine registration. Besides the necessity for the referencing within a single epoch, there is also a demand for linking different epochs to pave the way for monitoring purposes by means of temporal comparisons based on repeated measurements.

#### 3.1 Robotic multi-sensor system for plant monitoring

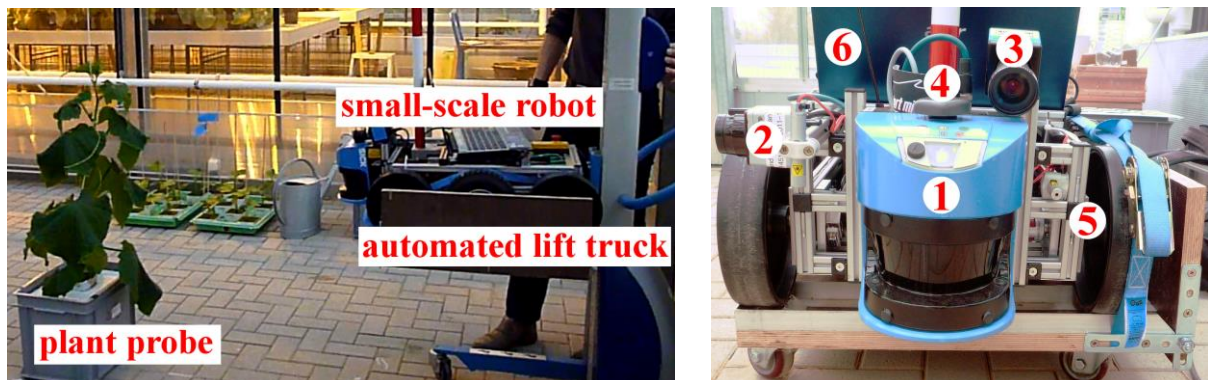


**Figure 1: Robotic multi-sensor system: Left: Side view of the acquisition situation in the green house with the small-scale robot on the automated lift truck to perform vertical movements. Right: Sensor pool installed on the small-scale robot: (1) SICK laser scanner, (2) Hokuyo laser scanner, (3) digital camera, (4) GPS aided MEMS based IMU, (5) small-scale robot and (6) consumer grade laptop.**

The core unit of the robotic multi-sensor system consists of two laser scanners: a SICK laser scanner of type LMS 500-20000 PRO-HR and a Hokuyo laser scanner of type URG-04LX. Both of them are 2D laser scanners which provide 2D scan lines. The raw measurements are polar coordinates (horizontal angles and ranges), which can be used to calculate Cartesian coordinates, and intensity values. The spatial resolution is defined by the angle increment used (0.1667 degree and 0.25 degree for the SICK and the Hokuyo laser scanner, respectively) and the distance to the object of typically 1 m. The sensor pool is completed by a digital camera (The Imaging Source DFK 41 with 1280x960 pixel) and a Global Positioning System (GPS) aided Micro-Electro-Mechanical Systems (MEMS) based Inertial Measurement Unit (IMU); in particular the XSens MTi-G is used. A small-scale robot (Volksbot RT6 by Fraunhofer IAIS) is acting as support platform for the sensors (cf. Figure 1 left). For in-depth information about the sensor's specifications, the reader is referred to the manufacturer's websites.

Essential for a multi-sensor platform is the proper synchronization of the data. At the moment, all sensors are connected to the same consumer grade notebook running the operating system Ubuntu 12.04 LTS with kernel 3.2.0-58-generic x86\_64. For the sensor control and data acquisition the Robot Operating System, Version Groovy Galapagos (QUIGLEY ET AL., 2009) is used. Thus for all different data sources the Unix time stamp is available. For a typical acquisition period of 30 seconds the Unix time stamp can be used. To be free of any clock errors or drifts the GPS time can be easily introduced as absolute and drift-free reference time for the multi-sensor system.

The SICK laser scanner is the main sensor for data acquisition of the plant probe. The laser scanner's laser beam is near-infrared (905 nm) with divergence of 4.7 mrad (4.7 mm diameter at 1 m distance). The manufacturer's datasheet provides a range accuracy of 12 mm at 6 m (object remission of 100%). The sensor is mounted with zero direction pointing towards the plant which yields horizontal scan lines for the plant under investigation. The third dimension results from motion, here vertical movement, of the entire robotic multi-sensor system. At the current developmental stage, an automated lift truck is used which allows operating heights of up to 1.7 m. The height changes are observed by the Hokuyo laser scanner whose zero direction is pointing towards the ground. To get the measure for the vertical motion, the data of a narrow angle range (nadir  $\pm 2^\circ$  angle increment of  $0.25^\circ$ ) of the Hokuyo laser scanner is used to get the height value above the ground. The 3D point cloud is generated by data fusion of the two laser scanners. The final height component for the SICK laser scanner's horizontal scan line is obtained by linear interpolation of the Hokuyo height values. It is noteworthy that only relative changes in height are of interest which does not demand for a rigorous determination of the mutual orientation of the two involved laser scanners.

In addition, a digital camera is mounted on top of the SICK laser scanner. The purpose of integrating a camera, providing Red-Green-Blue (RGB) data, into the robotic multi-sensor system is twofold. On the one hand, it can be used for visualization purposes; this means the colouring of the laser point clouds. On the other hand, these data can be valuable extra information in the segmentation procedure and provide details of the plant probe which are not visible in the laser point clouds.

The GPS aided MEMS based IMU is used to provide an absolute and drift-free reference time by the GPS time. In addition, the acceleration of gravity delivers useful data about the vertical movement of the robotic multi-sensor system. The 3D orientations (Euler angles) are currently not considered in the subsequent analysis. The GPS positions are not useable due to the indoor application. A synchronization of the different data sources of the multi-sensor platform can be assumed.

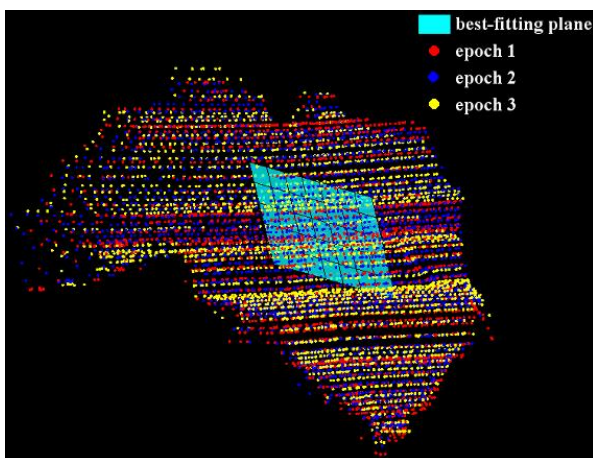


**Figure 2:** Accuracy assessment of the captured 3D point cloud. Exemplary leaf of a plant (18 cm in height and 23 cm in width) in three subsequent epochs (red, blue and yellow). The specific region under investigation is coloured cyan.

**Table 1:** Statistical values for an exemplary leaf of a plant in three subsequent epochs. Given are the minimal and maximal values of the residuals as well as their standard deviation for the cyan region in Figure 2.

|                | <i>min(res)</i> | <i>max(res)</i> | <i>std(res)</i> |
|----------------|-----------------|-----------------|-----------------|
| <i>epoch 1</i> | -12 mm          | 10 mm           | 4 mm            |
| <i>epoch 2</i> | -9 mm           | 7 mm            | 3 mm            |
| <i>epoch 3</i> | -12 mm          | 12 mm           | 4 mm            |

An accuracy assessment of the captured 3D point cloud is performed for a representative region of the acquired data (coloured cyan in Figure 2) in three subsequent epochs with an inter-epochal time span of 5 minutes. In each epoch, for this region of width and height of approx. 5 cm a best-fitting plane is estimated and statistical values for the remaining residuals are calculated. In Table 1 are given the minimal and maximal values as well as the standard deviation of the residuals. By these values can be concluded that the noise level of the acquired 3D point cloud data is within the sensors' specification.

### 3.2 Spatial referencing of individual survey positions within a single epoch

The referencing within a single epoch is supported by a well-chosen acquisition scheme (cf. Figure 3) which means that the survey positions of the multi-sensor platform are signaled on the ground floor. In addition, a point on the box (in which the plant is growing) is signaled to recover the orientation. By means of commercial laser pointers firmly attached to the robotic multi-sensor platform, the signaled points (light red circle in Figure 3) are sighted. This makes it possible to recover the survey position in terms of distance to the plant and angle segment roughly. Both values, distance and angle segment, can be interpreted as a priori transformation parameters within the coarse registration. Thus, the transformation of the three survey positions (typically used) into a common coordinate system with origin in the middle of the plant can be calculated. No further infrastructure besides the marked survey positions and the signaled points on the box are required for this coarse registration. But it has to be mentioned, that especially for temporal comparisons and repeated measurements this procedure is error prone. For a more reliable coarse registration the use of (at least three) artificial targets is proposed. This is the typical procedure in terrestrial laser scanning applications.

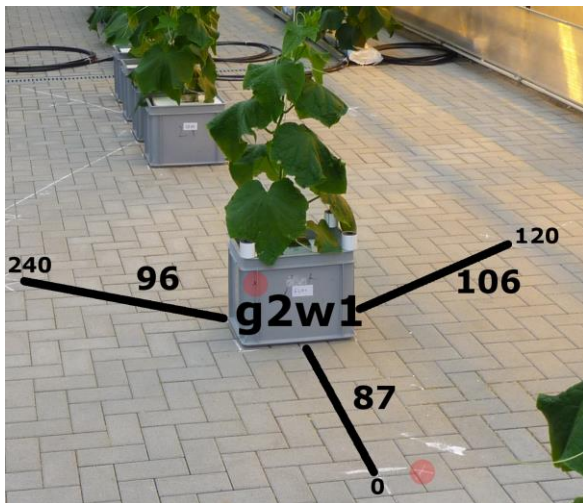


**Figure 3: Acquisition scheme with its three survey positions (angular step pattern of 120 degrees) for the plant under investigation. The two light red circles indicate the signaled points of survey position 0 degree to recover the a priori transformation parameters.**

The fine registration is done by iterative matching by means of an implementation of the iterative closest point algorithm (BESL & MCKAY, 1992). Since these kind of iterative matching algorithms are based on partially overlapping regions in the 3D point clouds, the aforementioned coarse registration is mandatory. The fine registration is done pair-wise with respect to, in general, the first survey position. Finally, for the entire plant probe a 3D point cloud in a common coordinate system is available. It has to be noted, however, that a certain time span exists between each data acquisition of the different survey positions. As each acquisition takes place in about 30 seconds, it can be assumed that the plant is not moving significantly during the acquisition process, so that the complete 3D point cloud can be interpreted as the point cloud of one epoch.

### 3.3 Temporal referencing of point clouds of different epochs

The temporal referencing of different epochs is based on the previously performed spatial referencing. To define a common coordinate system over time, stable areas in the spatially referenced data have to be identified. Like aforementioned, these can be artificial targets which are also usable in the coarse registration. One way is the use of cylindrical, retro-reflective targets which have to be additionally placed in the scanning area. Another convenient way proposed by HARMENING (2013) is the use of the box in which the plant grows.

The extraction of the box out of the 3D point cloud results in no extra task since this is already done in the spatial segmentation to separate the plant leaves in the box's surrounding. The segmented box is represented by four vertical planes and one horizontal plane (cf. Figure 4). The horizontal plane is given by the bottom side of a styrofoam element which is located on top of the box and consequently corresponds to the upper boundary of the box. As the Styrofoam element protrudes from the box, the transition from the box to the Styrofoam element is characterised by a significant change in the range values. It should be noted that only the position in z-direction and not the magnitude of the change in the range values is relevant to define the plane. Therefore, penetration effects of the horizontal laser can be neglected. The intersection of the four vertical planes and the one horizontal plane yield four common points which are indicated by yellow circles in Figure 4. To increase the reliability of the referencing, an additional point (white circles in Figure 4) for each common point is constructed. This is done by a defined shift in z-direction, which leads for the additional and common points to the same x- and y-coordinates and different z-coordinates. These eight points are suitable for reliable, temporal referencing by means of a 3D similarity transformation with three translation and three rotation parameters. Due to the use of a laser scanner the consideration of a scale parameter is not necessary. A result of the temporal referencing procedure is given in Figure 5. A measure for the correspondence of the two epochs under investigation is the mean coordinate error of the transformation. The mean coordinate error decreases from a value of 25 mm before to a value of 8 mm after the transformation. This remaining error is in the order of the range accuracy of the used laser scanner. Therefore, the establishment of a common coordinate system over time succeeded.

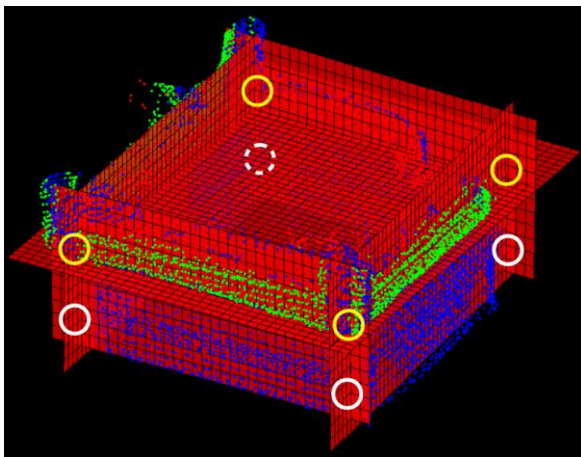


Figure 4: In red are depicted the extracted box elements; the yellow and white circles indicate the common points; blue colour indicates the point cloud and green stands the styrofoam element on top of the box.

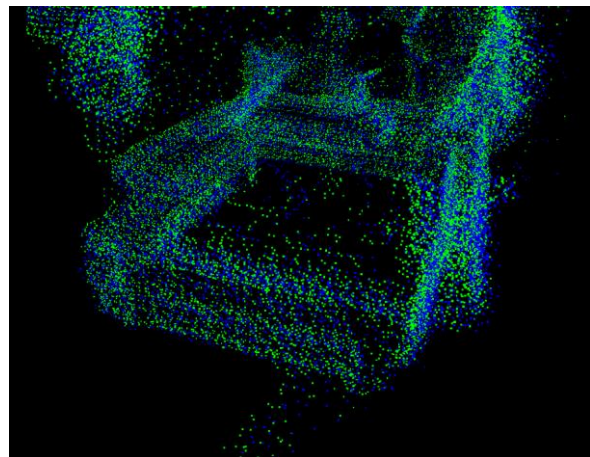


Figure 5: Results of the temporal referencing of two epochs coloured blue and green. The time span between the two epochs is about 18 minutes.

## 4 3D POINT CLOUD SEGMENTATION OF NATURAL PLANT OBJECTS

The first processing step for the analysis of a point cloud is the segmentation: According to a similarity measure the set of the so far unordered point cloud is partitioned into disjoint and connected subsets. In case of phenotyping this segmentation is identical with the grouping of points describing

the same plant organs. The segmentation of natural objects, in particular of plants, is a challenging task, which is caused by the varying appearances of plants as well as the complex structure of plants leading to occlusions and contacting leaves. These difficulties are the reasons why the use of generic segmentation algorithms is in general not satisfying. In this paper a segmentation algorithm is proposed, which consists of a graph based spatial segmentation as well as a following shape matching to segment the temporal dimension. Finally, this results in a spatiotemporal segmentation of the 3D point cloud.

## 4.1 Spatial segmentation

The basis for the spatial segmentation is the definition of a similarity measure. As different plant organs are very similar in their spectral properties but differ in their geometric properties, it is appropriate to use the latter as a segmentation basis. The fact that the geometric properties such as the curvature or the direction of the normal vary within the same leaf interfere this strategy. Therefore the adaptive segmentation criterion proposed by FELZENSZWALB & HUTTENLOCHER (2004) is used in the following:

Their algorithm interprets the input as a graph  $G = (V, E)$  consisting of nodes  $v_i \in V$  and undirected edges  $e_{ij} = \{v_i, v_j\} \in E$ , whose weights  $w_{ij}$  express the similarity of the connected nodes. Furthermore the algorithm operates according to the bottom up principle and therefore starts with an initial segmentation where each node corresponds to an individual segment. Based on this initial segmentation an edge list sorted in ascending order is constructed. Each of those edges is examined if an object boundary between the two connected nodes exists. Therefore, two values are evaluated: The internal difference  $Int(C)$  is a measure for the variation in the properties within the segment  $C$ . This value is defined as the maximum weight of the minimum spanning tree (MST) constructed by the points of  $C$ :

$$Int(C) = \max(w(e)) \quad \text{with } e \in \text{MST}(C, E). \quad (1)$$

The difference between two Segments  $Dif(C_1, C_2)$  represents the variation between the properties of the two segments  $C_1$  and  $C_2$  and is defined as the minimum of the weights belonging to all edges connecting  $C_1$  and  $C_2$ :

$$Dif(C_1, C_2) = \min(w_{ij}) \quad \text{with } v_i \in C_1, v_j \in C_2. \quad (2)$$

According to FELZENSZWALB & HUTTENLOCHER (2004) there is an evidence for an object boundary if

$$Dif(C_1, C_2) > \min( Int(C_1) + \tau(C_1), Int(C_2) + \tau(C_2) ) \quad \text{with } \tau(C) = \frac{k}{|C|}. \quad (3)$$

In this case  $C_1$  and  $C_2$  remain separated; otherwise the segments are merged. The level of over- or undersegmentation can be controlled by means of the threshold unit  $\tau(C)$  which is calculated from the segment's size  $|C|$  and a constant  $k$  which can be chosen freely initially: Large values of  $k$  lead to under- small values to oversegmentation.

Originally the introduced algorithm was developed with the objective of image segmentation. In order to transfer the idea to the segmentation of point clouds, it is necessary to define neighbourhoods in the point cloud. In this paper a radius search is used for this purpose.

As the separation of contacting leaves is the main challenge regarding the segmentation of plants, a reasonable choice of the similarity measure is required. In general, the transition between two contacting surfaces is indicated by a change in the normal direction. That is the reason why we propose the angle between the corresponding surface normals  $\mathbf{n}_i$  and  $\mathbf{n}_j$  to define the edge weights and by association the similarity measure:

$$w_{ij} = \arccos\left(\frac{\mathbf{n}_i^T \cdot \mathbf{n}_j}{|\mathbf{n}_i| \cdot |\mathbf{n}_j|}\right). \quad (4)$$

As the change of the normal direction within a leaf may be larger than the change of the normal direction between two contacting leaves, it is impossible to obtain a completely satisfying segmentation: Either the result is oversegmented or it is undersegmented. In this paper the parameter  $k$  is chosen to obtain an oversegmented result (cf. Figure 6), which forms the basis for a statistically based region merging. In this postprocessing two segments are either merged if they describe the same surface or if their border edges follow the same space curve. Both of these decisions are made by means of a statistical hypothesis test. For more details see HARMENING (2013).

The overall result of the spatial segmentation can be seen in Figure 7. Compared to Figure 6, the leaves are completely segmented and there do not exist any undersegmentations. Low point densities may cause oversegmentations, but in general the results are satisfying with respect to the subsequent phenotyping. It should be noted, however, that the result's quality depends strongly on the quality of the pre-segmentation, so that the value of the constant  $k$  has to be chosen carefully.

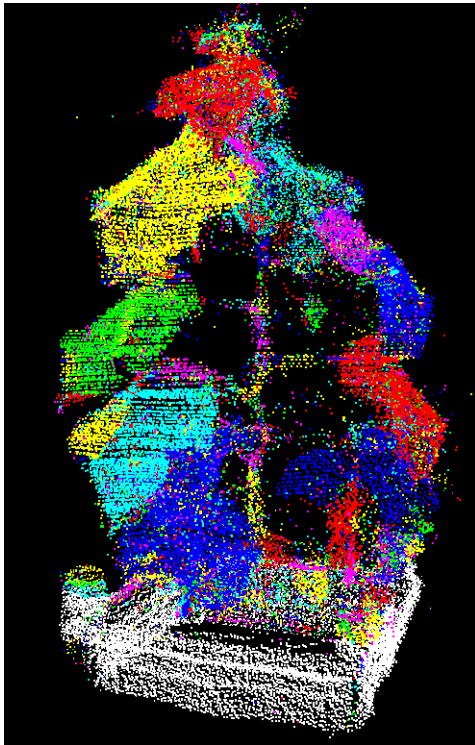


Figure 6: Oversegmented intermediate result: Various segments are coloured differently; points which do not belong to the plant are coloured white.

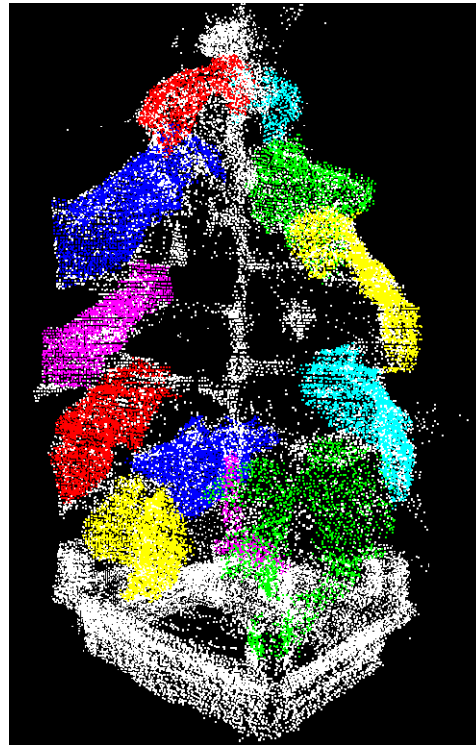


Figure 7: Overall result of the spatial segmentation: The leaves are coloured randomly, all points coloured in white belong to the error class.

## 4.2 Temporal segmentation by means of shape matching

The results obtained by means of the computations described in the previous section can be used to derive geometrical characteristics of the plants. In many cases it is required to determine the changes of these characteristics. In this case a time series of point clouds forms the basis to determine a segmentation which is consistent in time. In this paper the spatial and the temporal dimension are segmented successively. The tracking is realised by means of a shape matching algorithm, which identifies corresponding segments by their shape. This approach is motivated by the effect that a segment may split from one spatial segmentation to another (cf. Figure 8). Contrary to the centre of mass or the size for example, the shape of a segment is mostly unaffected by this effect. BRENDDEL &

TODOROVIC (2009) propose a shape matching algorithm based on dynamic time warping, which also forms the basis for the temporal segmentation in this paper.

Dynamic time warping (DTW) is a method originally used in speech recognition to align two sequences  $X = (x_1, x_2, \dots, x_n)$  and  $Y = (y_1, y_2, \dots, y_n)$  in an optimal manner. A cost function  $c(x_i, y_j)$  is used to express the effort for the alignment. Under all possible transformations the solution causing the minimal overall cost is the requested transformation. This optimization problem can be solved by means of dynamic programming as described in MÜLLER (2007).

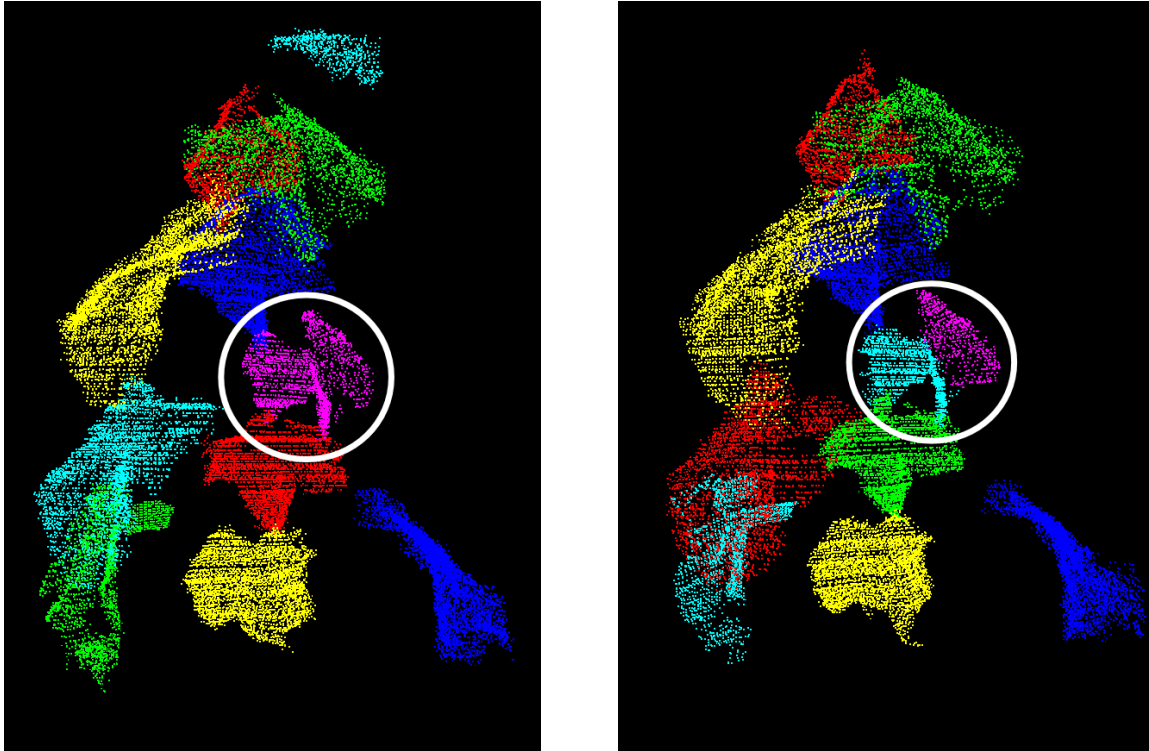


**Figure 8: Results of the spatial segmentation of two different point clouds of the same plant: The leaves are coloured randomly; no link exists between the same leaves so that equal colours of the same leaves arise by chance. The white circle indicates the effect that one segment may split from one spatial segmentation to another.**

In case DTW is used to identify corresponding segments in different point clouds, the segment edges are interpreted as sequences. The edges can be identified by means of a variant of the Douglas-Peucker-algorithm as described in HARMENING (2013). It should be noted, however, that these edges are cyclic sequences at first, which have to be split at an appropriate point. Afterwards the similarity of two such sequences can be evaluated by means of the overall warping cost required to perform the DTW.

The first step to perform the shape matching is the determination of possible matching partner: Assuming that a leaf's position as well as its shape remains approximately unchanged from one point cloud to another, the segments of one point cloud are interpreted as templates. For each template possible correspondences are determined using a radius search. Afterwards for each possible correspondence the normalised warping costs can be computed according to:

$$\bar{c}_{DTW} = \frac{c_{DTW}}{\min(n_1, n_2)} \quad (5)$$

In Equation (5) the overall warping cost  $c_{DTW}$  as well as the length of the sequences  $n_1$  and  $n_2$  are given. Given that exactly one matching partner to each template exists, the segment causing the smallest warping cost is the desired correspondence. Taking account of the oversegmentation, the

warping costs of combined segments are computed as well, while each segmented point cloud is alternately interpreted as a template. The result of these computations is a list containing possible correspondences from which the optimal correspondences are chosen by means of a greedy algorithm. The result of the shape matching, which is equivalent to the spatiotemporal segmentation, can be seen in Figure 9. On the one hand, all the leaves are tracked successfully over the time, which is indicated by means of the point cloud's coloration. On the other hand, it is possible to reduce the amount of oversegmentation taking into account the information provided by the spatial segmentations of the remaining point clouds of the time series. As a consequence the original spatial segmentation can be improved by means of the shape matching. Just as in the spatial segmentation, it has to be guaranteed, that the initial segmentations are not undersegmented.

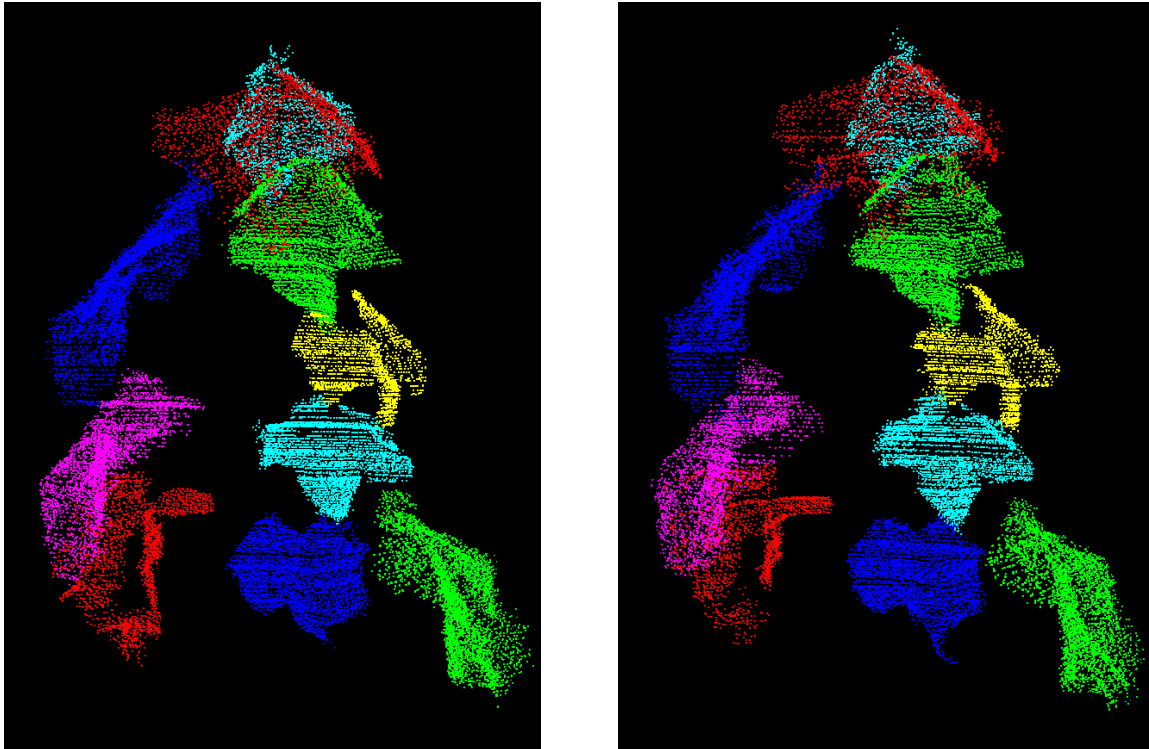


**Figure 9: Result of the spatiotemporal segmentation by means of the shape matching: After including temporal coherences there exists a link between the same leaves, so that the identical colour of the same leaves indicates a successful tracking. The time span between the two epochs is about 18 minutes.**

## 5 DISCUSSION AND OUTLOOK

The aims of this contribution can be summarized as the generation of time series for 3D point clouds showing natural objects in occluded scenes and as the spatiotemporal segmentation of the natural objects of interests, here cucumber plants, out of the 3D point cloud. In Figure 10 a result of the spatiotemporal segmentation for a data set with a time span of about 5 minutes between each epoch is shown. All 13 plant leaves are segmented and tracked over time successfully which is indicated by the identical colour. In white colour plant parts besides the leaves are given, typically these parts correspond to the plant stem.

The use of the introduced robotic multi-sensor system for the data acquisition and the required subsequent mutual referencing of different survey positions worked well in the occluded environment of cucumber plants under canopy conditions. Even the temporal referencing could be solved without the demand for extra targets in an automated processing sequence. Nevertheless, the drawback of low point densities in certain parts of the 3D point clouds has to be mentioned. Especially in the spatial segmentation this effect leads to oversegmentations. There are two reasons for the low point densities: On the one hand, the mutual occlusions of leaves result in low point densities which can be solved by additional and well chosen extra survey positions. On the other hand, the horizontal orientation of the

SICK laser scanner with respect to the ground floor yields low point densities especially for near vertical leave surfaces. This problem will be faced in ongoing experiments by a slight adaption of the orientation of the laser scanner. Finally should be noted, that for all data sets undersegmentations could be avoided, which means that the main challenge – the separation of contacting leaves – could be solved.

The spatiotemporal segmentation of the cucumber plants under investigation succeeded for time spans of subsequent epochs in minute up to hour level. Thus the estimated leave movements and deformations are of small magnitude. These short time spans pave the way for identification of corresponding leaves by means of their shape. The establishment of a temporal link between same leaves of different epochs (temporal segmentation) also supports the spatial segmentation in case of split segments. Current limitations of the proposed approach are time spans of about 10 days and more. Here, the shape of the leaves changes in a way that the shape matching yields insufficient results. It should be noted that such time spans can be analysed if adequate intermediate acquisitions with hour to day level are considered. This overcomes the limitation of the abovementioned relative short time spans. Since the data acquisition and analysis can be performed semi-automatic the extra work caused by intermediate steps is not significant. A topic of further investigations will be the analysis regarding maximal time spans for a successful shape matching. In addition, our future work will concentrate on estimating values for the leave area which requires in general a proper triangulation of the 3D point cloud. Therefore, first experiments with the use of alpha shapes (HARMENING, 2013) will be picked up and refined.

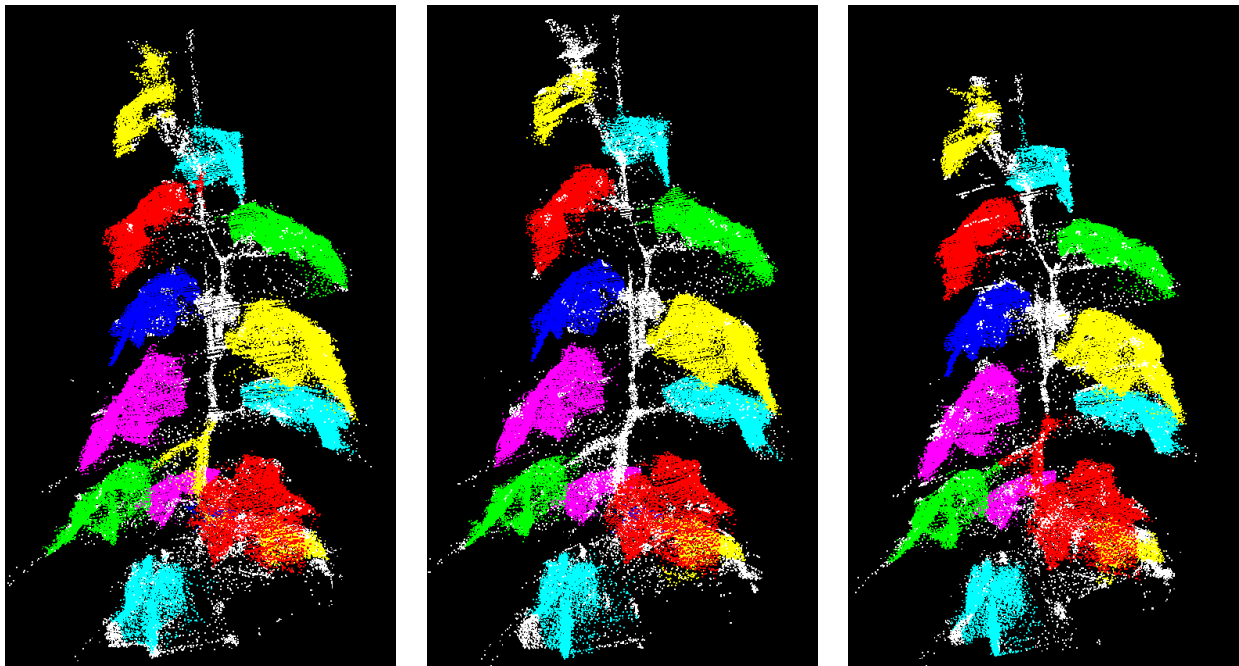


**Figure 10: Results of the spatiotemporal segmentation over three epochs. The identical colour of the same leaves indicates a successful tracking. Plant parts besides the leaves are coloured white. The time span between two epochs is about 5 minutes.**

## ACKNOWLEDGEMENTS

The first author acknowledges the financial support by the *Leibniz Universität Hannover* for the funding of the project *Raum-zeitlich dichtes Monitoring von Pflanzenbeständen mittels Messroboter* within the scope of the program *Wege in die Forschung II - Projektförderung für junge Wissenschaftler/-innen* in the period March 2013 to February 2014. The presented research work was done while the first author J.-A. Paffenholz was with the Institute of Cartography and Geoinformatics (ikg), Leibniz Universität Hannover. The second author C. Harmening was also with the ikg for her Master thesis. All experiments were carried in the scope of the mentioned project and in cooperation

with the *Institute for Horticultural Production Systems, Leibniz Universität Hannover*. Therefore, the authors acknowledge the support given by the Head of the Section *Vegetable Systems Modelling* Prof. Dr. Hartmut Stützel, Christian Wagner and Dr. Dirk Wiechers, who is now with KWS Saat AG, Einbeck.

## REFERENCES

- ALENYA, G.; DELLEN, B. & TORRAS, C.: *3D modelling of leaves from color and ToF data for robotized plant measuring*. In: 2011 IEEE International Conference on Robotics and Automation. ICRA. Shanghai, China: IEEE Xplore Digital Library, S. 3408–3414, 2011.
- BESL, P. J. & MCKAY, N. D.: *A method for registration of 3-D shapes*. In: *IEEE Trans. Pattern Analysis and Machine Intelligence* **14** (2), S. 239-256, 1992.
- BRENDEL, W. & TODOROVIC, S.: *Video object segmentation by tracking regions*. In: 2009 IEEE 12th International Conference on Computer Vision (ICCV). ICCV. Kyoto, 21 September - 2 October, S. 833–840, 2009.
- BUSEMEYER, L.; MENTRUP, D.; MÖLLER, K.; WUNDER, E.; ALHEIT, K.; HAHN, V. et al.: *BreedVision — A multi-sensor platform for non-destructive field-based phenotyping in plant breeding*. In: *Sensors* **13** (3), S. 2830–2847, 2013.
- FELZENSZWALB, P. F. & HUTTENLOCHER, D. P.: *Efficient Graph-Based Image Segmentation*. In: *International Journal of Computer Vision* **59** (2), S. 167–181, 2004.
- FIORANI, F. & SCHURR, U.: *Future scenarios for plant phenotyping*. In: *Annu Rev Plant Biol* **64**, S. 267–291, 2013.
- GORTE, B. & PFEIFER, N.: *Structuring Laser-scanned Trees Using 3D Mathematical Morphology*. In: Orhan Altan (Hg.): XXth ISPRS Congress, Technical Commission V. XXth ISPRS Congress. Istanbul, 12-23 July. Istanbul (ISPRS International Archives of the Photogrammetry, Remote Sensing and Spatial Information Sciences, XXXV-B5), S. 929–933, 2004.
- GORTE, B. & WINTERHALDER, D.: *Reconstruction of Laser-Scanned Trees Using Filter Operations in the 3D Raster Domain*. In: M. Thies, B. Koch, H. Spiecker und H. Weinacker (Hg.): Laser-Scanners for Forest and Landscape Assessment, 36(8/W2). Laser-Scanners for Forest and Landscape Assessment. Freiburg, 3-6 October. International Society for Photogrammetry and Remote Sensing (ISPRS): Freiburg (ISPRS International Archives of the Photogrammetry, Remote Sensing and Spatial Information Sciences, XXXVI-8/W2), S. 39–44, 2004.
- HARMENING, C.: *Raum-zeitliche Segmentierung von natürlichen Objekten in stark verdeckten Szenen*. Master thesis (unpublished). Leibniz Universität Hannover, Hannover. Institut für Kartographie und Geoinformatik, 2013.
- HOFFMEISTER, D.; TILLY, N.; BENDIG, J.; CURDT, C. & BARETH, G.: *Detektion von Wachstumsvariabilität in vier Zuckerrübensorten durch multi-temporales terrestrisches Laserscanning*. In: Michael Clasen (Hg.): Informationstechnologie für eine nachhaltige Landwirtschaft. Referate der 32. GIL-Jahrestagung. Freising, 29.03 - 01.04. Bonn: Gesellschaft für Informatik (GI-Edition : Proceedings, 194), S. 135–138, 2012.
- HÖFLE, B.: *Radiometric Correction of Terrestrial LiDAR Point Cloud Data for Individual Maize Plant Detection*. In: *IEEE Geosci. Remote Sensing Lett.*, S. 1–5, 2013.
- KAHLEN, K. & STÜTZEL, H.: *Estimation of Geometric Attributes and Masses of Individual Cucumber Organs Using Three-dimensional Digitizing and Allometric Relationships*. In: *J. Amer. Soc. Hort. Sci.* **132** (4), S. 439–446, 2007.
- KLOSE, R.; PENLINGTON, J. & RUCKELSHAUSEN, A.: *Usability study of 3D Time-of-Flight cameras for automatic plant phenotyping*. In: Manuela Zude (Hg.): Image Analysis for Agricultural Products and Processes. Potsdam-Bornimer, 27-28 August. Leibniz-Institut für Agrartechnik Potsdam-Bornim e. V. (Bornimer Agrartechnische Berichte, 69), S. 93–105, 2009.
- MÜLLER, Meinard: *Information retrieval for music and motion*. New York: Springer, 2007.

- NORZAHARI, F.; FAIRLIE, K.; WHITE, A.; LEACH, M.; WHITTY, M.; COSSELL, S. et al.: *Spatially Smart Wine - Testing geospatial technologies for sustainable wine production*. In: Proceedings of the FIG Working Week 2011. Bridging the Gap between Cultures. Marrakech, 18-22 May. FIG, S. 19, 2011.
- PAPROKI, A.; SIRAUT, X.; BERRY, S.; FURBANK, R. & FRIPP, J.: *A novel mesh processing based technique for 3D plant analysis*. In: *BMC Plant Biol* **12** (1), S. 63–75, 2012.
- PAULUS, S.; DUPUIS, J.; MAHLEIN, A.-K. & KUHLMANN, H.: *Surface feature based classification of plant organs from 3D laserscanned point clouds for plant phenotyping*. In: *BMC Bioinformatics* **14** (1), S. 238, 2013.
- QUIGLEY, M.; GERKEY, B.; CONLEY, K.; FAUST, J.; FOOTE, T.; LEIBS, J. et al.: *ROS: an open-source Robot Operating System*. In: Open-Source Software workshop of the International Conference on Robotics and Automation. Open Source Software in Robotics, ICRA. Kobe, 17 May, 2009.
- ROSELL, J. R.; LLORENS, J.; SANZ, R.; ARNÓ, J.; RIBES-DASI, M.; MASIP, J. et al.: *Obtaining the three-dimensional structure of tree orchards from remote 2D terrestrial LIDAR scanning*. In: *Agricultural and Forest Meteorology* **149** (9), S. 1505–1515, 2009.
- SANZ-CORTIELLA, R.; LLORENS-CALVERAS, J.; ESCOLÀ, A.; ARNÓ-SATORRA, J.; RIBES-DASI, M.; MASIP-VILALTA, J. et al.: *Innovative LIDAR 3D Dynamic Measurement System to Estimate Fruit-Tree Leaf Area*. In: *Sensors* **11** (6), S. 5769–5791, 2011.
- SEATOVIC, Dejan: *Methods for Real-Time Plant Detection in 3-D Point Clouds*. PhD thesis. München: DGK (Reihe C, 704), 2013.
- SELBECK, J.; DWORAK, V. & EHLERT, D.: *Datenerfassung aktueller Bestandsparameter mittels eines fahrzeuggestützten LiDAR Scanners*. In: Wilhelm Claupein und Ludwig Theuvsen (Hg.): Precision agriculture reloaded - informationsgestützte Landwirtschaft. Referate der 30. GIL Jahrestagung. Stuttgart, 24 - 25 Februar. GIL conference; GIL-Jahrestagung; Jahrestagung der Gesellschaft für Informatik in der Land-, Forst- und Ernährungswirtschaft. Bonn: Gesellschaft für Informatik (GI-Edition Proceedings, 158), S. 179–182, 2010.
- SUN, Z.; LU, S.; GUO, X. & TIAN, Y.: *Leaf Vein and Contour Extraction from Point Cloud Data*. In: 2011 International Conference on Virtual Reality and Visualization: IEEE, S. 11–16, 2011.
- UHRMANN, F.; SEIFERT, L.; SCHOLZ, O.; SCHMITT, P. & GREINER, G.: *Improving Sheet-of-Light Based Plant Phenotyping with Advanced 3-D Simulation*. In: Albert Heuberger, Günter Elst und Randolph Hanke (Hg.): Microelectronic systems. Circuits, systems and applications. Berlin: Springer, S. 247–257, 2011.
- WHITE, J. W.; ANDRADE-SANCHEZ, P.; GORE, M. A.; BRONSON, K. F.; COFFELT, T. A.; CONLEY, M. M. et al.: *Field-based phenomics for plant genetics research*. In: *Field Crops Research* **133**, S. 101–112, 2012.

Contact:

Dr.-Ing. Jens-André Paffenholz,  
Geodetic Institute, Leibniz Universität Hannover  
Nienburger Str. 1, D-30167 Hannover, Germany  
phone: +49 (0511) 762-3191  
Email: paffenholz@gih.uni-hannover.de